

# Bismuth-substituted Lutetium Iron Garnet Films with Giant Visible-Range Magneto-Optical Sensitivity

Megan H. Dransfield, Lukáš Flajšman,<sup>a)</sup> Matthijs H. J. de Jong, Sebastiaan van Dijken, and Laure Mercier de Lépinay<sup>b)</sup>

*Department of Applied Physics, Aalto University, FI-00076, Finland*

(Dated: 24 February 2026)

Magneto-optical materials are indispensable across modern physics, serving as the foundation for precision magnetic sensing, nonreciprocal photonics, and optical isolation technologies. The continual pursuit of materials with high Verdet constants has driven the development of garnet-based compounds exhibiting extreme magneto-optical sensitivity. In this work, we report the growth and comprehensive magneto-optical characterization of bismuth-substituted lutetium iron garnet (LuBiIG), a material that combines the large spin-orbit coupling of bismuth with the lattice stability of lutetium iron garnet. The films exhibit an exceptionally high Verdet constant of up to  $-0.120^\circ \mu\text{m}^{-1} \text{mT}^{-1}$ , peaking in the visible spectral range near 520 nm. LuBiIG films with thicknesses between 80 and 220 nm were grown by pulsed laser deposition and characterized at room temperature over the 500 nm to 820 nm wavelength range. These results position LuBiIG as a highly sensitive magneto-optical material suitable for advanced cryogenic detection and hybrid quantum applications.

The development of highly sensitive magneto-optical materials is essential for imaging and detecting nanoscale magnetic textures and weak magnetic fields, including magnetic domains, skyrmions, and flux structures in superconductors<sup>1-3</sup>. Beyond fundamental studies, such materials underpin technological applications ranging from high-density magnetic recording<sup>4-6</sup> to optical isolators and nonreciprocal photonic components<sup>7,8</sup>. Over the past decades, extensive research has explored various rare-earth and transition-metal garnets, enhancing available magneto-optical sensitivity and spectral tunability. Building upon these advances, our primary goal is to realize films optimized for quantitative magneto-optical imaging. In magneto-optical detection, linearly polarized light interacts with a magnetized transparent medium, and its polarization is rotated by the Faraday or Kerr effect. The magnitude of this rotation directly encodes the local magnetic field distribution, providing a powerful, non-invasive means to map out magnetic textures.

Substituted or doped garnet films combine strong magneto-optical coupling, high transparency, and large magnetic permeability<sup>9</sup>. These characteristics make them uniquely suited for high-resolution optical magnetometry and magneto-optical indicator films. Numerous studies have shown that the magneto-optical performance of garnets can be greatly enhanced by rare-earth or heavy-element substitution<sup>10-12</sup>. Among these, bismuth is a particularly promising dopant: its strong spin-orbit coupling increases the Faraday rotation almost linearly with concentration. Yet, the fabrication of bismuth-substituted iron garnets remains challenging due to the volatility of bismuth and its sensitivity to growth conditions. To produce such materials, most previous studies have relied on liquid-phase epitaxy (LPE), which yields excellent crystalline quality but often leads to film cracking and non-uniform bismuth incorporation<sup>13</sup>, both of which de-

grade magneto-optical performance. To overcome these limitations, pulsed laser deposition (PLD) can be used as a versatile, nonequilibrium technique capable of preserving target stoichiometry and enabling precise control over oxygen pressure and growth rate. This approach maintains the desired bismuth concentration while ensuring smooth, crack-free epitaxial films.

Bismuth-lutetium iron garnets (LuBiIG) have been recognized for several decades for their exceptionally high Verdet constants, and reduced absorption in the near-infrared range<sup>14,15</sup>, with the Faraday rotation reaching as high as  $4.8 \times 10^6$  °/m<sup>16</sup> at 633 nm. From the data recorded in this paper, we report rotation as high as  $6.2 \times 10^6$  °/m at 630 nm. The enhancement originates from diamagnetic electronic transitions between the ground and triply degenerate excited states, which strongly modify the permittivity tensor, as well as from crystal-field-induced transitions within the Fe sublattices<sup>17</sup>. Meanwhile, lutetium substitution alleviates lattice mismatch between Bi:Fe garnet and gadolinium gallium garnet (GGG) substrates, stabilizing epitaxial growth and ensuring stoichiometric fidelity<sup>18</sup>. Additionally, these materials have demonstrated sensitivity down to cryogenic temperatures (4 K)<sup>19</sup>. Together, these mechanisms make LuBiIG a prime candidate for high-sensitivity magneto-optical imaging possibly at even lower temperatures. We envisage to apply such materials to image magnetic flux in low-temperature superconductors where this has not yet been realized.

In this context, this work focuses on developing LuBiIG films using PLD, that would be suited in particular for the imaging of nanoscopic superconducting vortices hosting quantized magnetic flux that penetrates type-II superconductors, as this material has been shown to conserve its sensitivity at low temperatures for such applications<sup>19</sup>. For this application, the films would be mounted in a flip-chip stack with magnetic (or superconducting) samples allowing for an approach within 200 nm–1 μm of magnetic structures. To detect stray vortex fields of the order of 1 mT or less, the magneto-optical sensor must be highly sensitive. Moreover, to resolve single vortices, the film thickness should ideally be compar-

<sup>a)</sup>Electronic mail: [lukas.flajsman@aalto.fi](mailto:lukas.flajsman@aalto.fi)

<sup>b)</sup>Electronic mail: [laure.mercierdelepinay@aalto.fi](mailto:laure.mercierdelepinay@aalto.fi)

ble to the magnetic-field attenuation length of a vortex, typically around 100 nm for superconductors in the thin film limit. This paper reports on the growth and characterization of stable and crystalline LuBiIG films of thickness 80-220 nm with ultra-high Verdet constants, fulfilling the conditions on film thickness and sensitivity required to realize cryogenic magneto-optical microscopy of vortex textures with unprecedented spatial precision. The investigation studies the influence of growth parameters on the quality of these sensors and characterizes the magnetic and magneto-optical response at room temperature.

In preparation for film growth, (111)-oriented GGG substrates ( $5 \times 5 \times 0.5 \text{ mm}^3$ ) were ultrasonically cleaned in acetone and isopropanol and pre-annealed at  $1000^\circ\text{C}$  for four hours in flowing oxygen. This treatment significantly improves film surface quality and promotes growth-reproducibility.

Targets of composition  $\text{Bi}_{2.1}\text{Lu}_{0.9}\text{Fe}_5\text{O}_{12}$  were employed in a commercial PLD setup. PLD parameters have been previously explored for relatively similar target compositions<sup>20</sup>, although with almost reverse Bi:Lu stoichiometry. We nevertheless used these parameters as a starting point. Films (see Table I for the complete list) were deposited using a KrF excimer laser (248 nm) operating at a fluence of  $2.5 \text{ J cm}^{-2}$  and a repetition rate of 5 Hz. The substrate temperature during deposition was systematically varied between 650 and  $850^\circ\text{C}$ , while the oxygen background pressure ranged from 0.025 to 0.15 mbar. Each film (sample 1 to 8) was obtained by 15,000–25,000 laser pulses, yielding thicknesses in the range of 80–220 nm.

Following deposition, the samples were either cooled *in situ* at the growth pressure or subjected to post-annealing in 100 mbar of oxygen for 30 minutes. The annealing atmosphere was selected based on the crystalline quality observed during growth by reflection high-energy electron diffraction (RHEED). Films displaying sharp, streak-like RHEED patterns indicative of two-dimensional (2D) layer-by-layer growth were cooled directly at the deposition pressure, while those showing diffuse or spot-like three-dimensional (3D) diffraction features underwent an additional oxygen-rich anneal to promote crystallization and surface smoothening. All samples were subsequently cooled to room temperature at a controlled rate of  $5^\circ\text{C min}^{-1}$ . The final RHEED patterns recorded after cooldown (see Table I) provided a reliable assessment of the film morphology and crystalline order. Energy-dispersive X-ray spectroscopy (EDS) confirmed that the stoichiometry of the target was maintained during deposition.

The film thicknesses were measured using a stylus profilometer (Bruker DektakXT) to obtain accurate step-height profiles. During deposition, a narrow section of each substrate was masked by a metal clamp, preventing film growth and thereby creating a sharp step edge that served as a zero-thickness reference. After deposition, the clamp was removed and the step height was scanned along several 2 mm-long line profiles using a stylus force of 3 mN and a lateral resolution of  $0.1 \mu\text{m}$ . The resulting profiles confirmed uniformity of the LuBiIG films across the substrate. Thickness values extracted

Sample	Growth T ( $^\circ\text{C}$ )	Growth P (mbar)	Cooldown P (mbar)	Pulses x1000	RHEED pattern	$t$ (nm)
1	850	0.025	100	15	3D	164
2	750	0.025	0.025	25	3D	218
3	650	0.025	100	15	2D+3D	86
4	850	0.1	0.1	15	2D	84
5	750	0.1	0.1	15	2D	86
6	650	0.1	0.1	15	2D+3D	94
7	750	0.15	0.15	15	2D	91
8	650	0.15	100	15	2D+3D	108

TABLE I. Growth-related parameters for LuBiIG films grown by pulsed laser deposition on GGG substrates in  $\text{O}_2$  atmosphere, along with the observed post-growth RHEED diffraction signatures indicating the crystalline quality of each film. The last column indicates the thickness  $t$  obtained by stylus profilometry.

from these measurements are summarized in Table I. This direct mechanical method provided a robust calibration of the deposition rate.

The magnetic properties of the LuBiIG films were characterized using longitudinal magneto-optical Kerr effect (MOKE) magnetometry in a nearly-crossed polarizer configuration. A continuous-wave 405 nm laser was incident on the sample at an angle of  $45^\circ$ , and the reflected intensity was recorded as a function of the applied in-plane magnetic field. The plane of incidence and reflection was aligned along the in-plane crystallographic  $[1\bar{1}0]$  direction of the GGG substrate.

Magnetic hysteresis curves are shown in Fig. 1: all films exhibit low saturation fields in the in-plane direction which is consistent with the compressive strain expected for LuBiIG grown epitaxially on GGG(111)<sup>18</sup>. The magnitude of the in-plane saturation and coercive fields varies notably across the sample series, reflecting differences in crystalline quality and oxygen stoichiometry. Samples showing sharp, streak-like 2D RHEED patterns indicative of regular layer-by-layer growth display narrow, square hysteresis loops with low coercive fields of a few millitesla. In contrast, films exhibiting mixed or diffuse 3D RHEED features show broader, slanted loops with higher coercivity and increased saturation fields, characteristic of enhanced pinning and structural disorder. These correlations confirm that optimized oxygen pressure and improved crystalline order yield magnetically softer LuBiIG films with coherent domain reversal conditions.

Complementary to the optical magnetometry measurements, the saturation magnetization of each LuBiIG film was determined by vibrating sample magnetometry (VSM) under an in-plane magnetic field. The resulting saturation magnetization values using the measured film dimensions, are listed in Table II. The measured saturation magnetization correlates approximately with the crystalline quality of the samples, assessed by RHEED: a high crystalline quality (evidenced by a pattern typical of 2D structures) produces a larger magnetization value.

The spectral magneto-optical response of the LuBiIG films was characterized using normal-incident linearly polarized light. A supercontinuum laser (NKT SuperK EXW-12) combined with an acousto-optic tunable filter provided a contin-

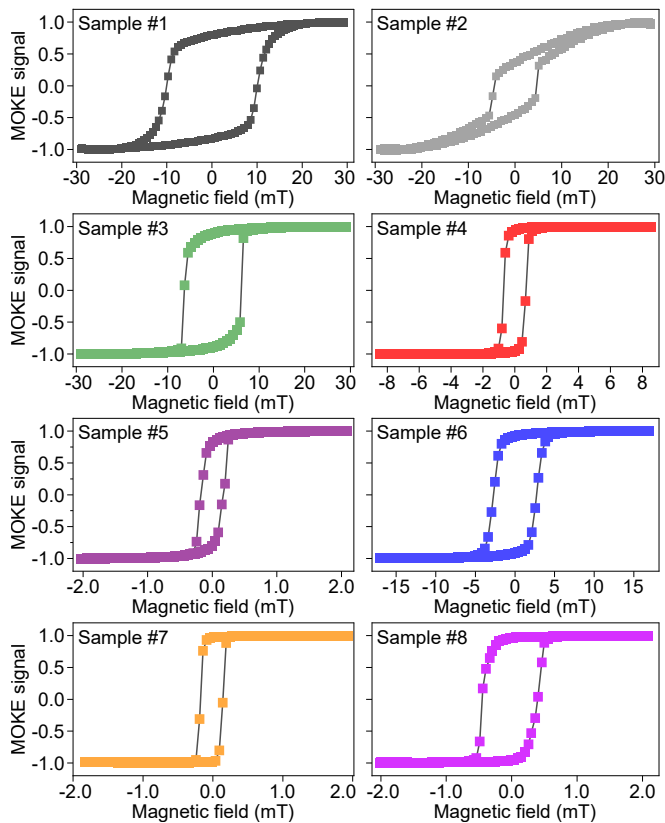


FIG. 1. Longitudinal MOKE hysteresis loops for the series of Lu-BiIG samples. Each curve is normalized to its maximum intensity. Note that the magnetic field range (x-axis) differs between panels to highlight the variation in saturation behavior.

uously tunable wavelength range from 500 nm to 1100 nm. The beam was passed through a high-extinction-ratio linear polarizer and directed onto the sample, which was positioned between the poles of an electromagnet generating an out-of-plane magnetic field. Both the transmitted and reflected light were measured simultaneously to quantify the Faraday and Kerr effects.

Photoelastic modulators (PEMs) operating at 50 kHz were placed in the transmitted and reflected paths to impose a high-frequency polarization modulation. The resulting optical signals were demodulated using lock-in detection at the first and second harmonics of the modulation frequency. The first harmonic corresponds to the ellipticity component, while the second harmonic encodes the polarization rotation. The transmitted and reflected beams were subsequently separated into their orthogonal linear components using polarizing beam splitters, and each polarization was detected by an independent photodiode. Using the PEM reference signal as the lock-in amplifier input allowed precise extraction of both rotation and ellipticity amplitudes<sup>21,22</sup>. This approach provides high sensitivity, enabling detection of sub-milliradian polarization changes across the full visible-near-infrared range. A calibrated out-of-plane magnetic field was applied to the samples and swept in magnitude to characterize their magneto-optical responses. The magneto-optical spectrome-

try setup was calibrated using a commercial magneto-optical sensor with a known magneto-optical response (Matesys sensor type B).

The absolute magnitude of the magneto-optical rotation was independently verified using a rotating-analyzer polarimeter (RAP) equipped with a motorized analyzer stage. For each magnetic field step, the analyzer was rotated around the extinction position within a  $\pm 5^\circ$  angular range. The resulting transmission intensity was recorded as a function of analyzer angle, and the position of the minimum in each trace was used to determine the sample-induced polarization rotation. The rotation values obtained from the RAP measurements showed excellent agreement with those acquired using the PEM-based detection system, confirming the accuracy of the magneto-optical calibration.

Figure 2(a) shows a representative Faraday rotation hysteresis loop of sample 8 measured at a wavelength of 600 nm. The raw signal includes contributions from both the LuBiIG film and the GGG substrate, the latter exhibiting a weak, linear magneto-optical response arising from its paramagnetic behaviour. To isolate the intrinsic film response, the independently measured GGG curve was subtracted from the data, effectively removing the linear substrate response and correcting the small zero-field offset attributed to instrumental artifacts. The out-of-plane Faraday rotation curves of all samples exhibit a nearly linear approach to saturation with narrow hysteresis and much higher saturation fields than under in-plane fields (of the order of some 100 mT), consistent with a hard-axis magnetic response. Linear fits of the linear domain and saturation plateaus were used to determine the saturation fields and the maximum Faraday rotation. The saturation fields averaged over all measured wavelengths are summarized in Table II, with uncertainties corresponding to the standard deviation of the wavelength-dependent fits.

Sample	OOP sat. field (mT)	Max Verdet const. ( $^\circ/\mu\text{m}/\text{mT}$ )	Max rotation ( $\times 10^7$ $^\circ/\text{m}$ )	$\mu_0 M_s$ (mT)
1	$150 \pm 54$	-0.109	1.8	228
2	$206 \pm 5$	-0.048	2.0	330
3	$234 \pm 4$	-0.103	3.0	662
4	$347 \pm 7$	-0.062	2.5	785
5	$229 \pm 9$	-0.106	2.7	537
6	$304 \pm 13$	-0.067	2.4	597
7	$349 \pm 7$	-0.062	2.6	1100
8	$180 \pm 4$	-0.120	2.1	512

TABLE II. Summary of characterization results: Out-of-plane (OOP) saturation field, maximum Verdet constant (within the wavelength range of 520–530 nm), maximum Faraday rotation, and saturation magnetization extracted from VSM measurements.

The slopes of the Faraday rotation curve determine the magneto-optical sensitivity of the LuBiIG films. To quantify this sensitivity under the low magnetic fields that are essential for magnetic-flux imaging in low-temperature superconductors, the electromagnet and samples were first demagnetized using a decreasing alternating magnetic field and the measurements were repeated over a reduced magnetic field range

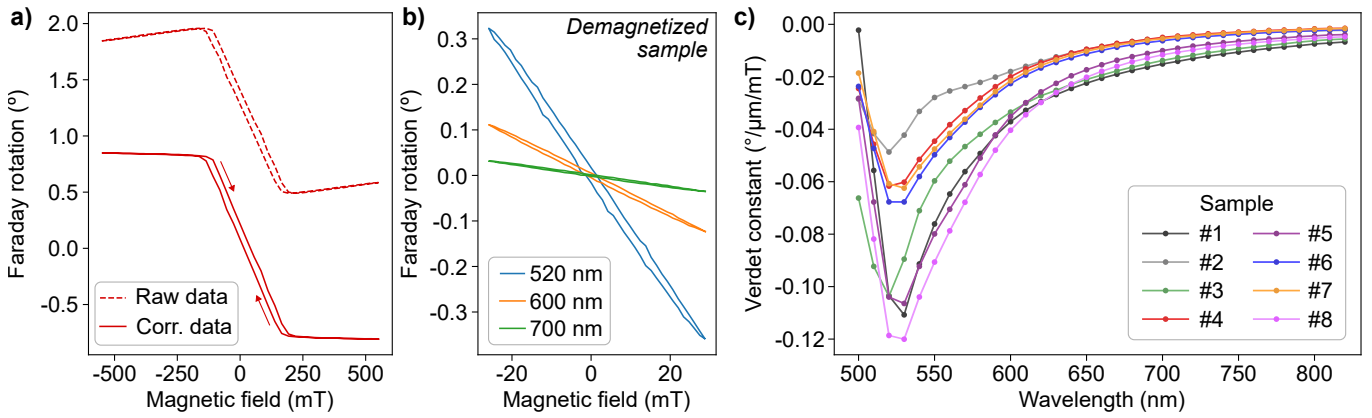


FIG. 2. (a) Representative Faraday hysteresis loop of sample 8 measured at a wavelength of 600 nm. The contribution from the GGG substrate is subtracted from the raw data (dashed red line), and the linear regions of the corrected curve (solid red line) are fitted to extract the saturation field. (b) Repeated hysteresis measurements at several wavelengths on a demagnetized sample over a reduced field range. The fitted slope is used to determine the Verdet constant. (c) Wavelength dependence of the Verdet constant for all LuBiIG films, exhibiting a pronounced maximum in absolute value at 520–530 nm.

well below saturation. Over this smaller magnetic field range, the magneto-optical response is linear as shown in Fig. 2(b), that is, the polarization rotation  $\theta$  is a linear function of the magnetic flux density  $B$ , and it presents almost no hysteresis, allowing precise extraction of the sensitivity as the slope of this linear function. The Verdet constant  $V$  is then calculated  $V = \frac{1}{t} \frac{\partial \theta}{\partial B}$  where  $t$  is the thickness of the film reported in table I. The values of the Verdet constants of all LuBiIG films are plotted as a function of wavelength in Fig. 2(c), showing that the magneto-optical sensitivity peaks sharply at 520–530 nm. This maximum corresponds to electronic transitions involving hybridized Bi  $6p$ –O  $2p$ –Fe  $3d$  states, which enhance spin-orbit coupling and produce a strong dispersion in the magneto-optical response<sup>10,14,23</sup>. As a result, employing standard solid-state lasers with the common wavelength of 532 nm would yield near-optimal sensitivity for magneto-optical detection.

Table II summarizes the peak Verdet constants for all samples, which significantly exceed the values typically reported for conventional iron garnets<sup>24</sup> and rank among the highest achieved for LuBiIG thin films<sup>19,25</sup>. The largest Verdet constants are observed for samples 1 and 8 ( $-0.109^\circ \mu\text{m}^{-1} \text{mT}^{-1}$  and  $-0.120^\circ \mu\text{m}^{-1} \text{mT}^{-1}$ , respectively), which also exhibit the lowest magnetic saturation fields, confirming the correlation between structural quality, magnetic softness, and magneto-optical sensitivity.

In summary, films of LuBiIG were grown on (111)-oriented GGG substrates using pulsed laser deposition. Optimizing the growth temperature, oxygen pressure, and post-annealing conditions produced crack-free epitaxial layers with preserved stoichiometry and thicknesses between 80 and 220 nm. The Faraday effect measured for wavelengths between 500 and 800 nm revealed a pronounced wavelength dependence with a distinct maximum near 520–530 nm, associated with Bi–O–Fe hybridized electronic transitions that strongly enhance spin-orbit coupling<sup>10,14,23</sup>.

The largest Verdet constant in magnitude reached  $-0.120^\circ \mu\text{m}^{-1} \text{mT}^{-1}$ , placing these films among the most

magneto-optically active materials ever reported. This value surpasses typical magneto-optical garnets by more than an order of magnitude<sup>24</sup> and rivals the record performance of the best LuBiIG thin films in the literature<sup>19,25</sup>. The largest constants were achieved in samples annealed in 100 mbar of oxygen, which also exhibited the lowest magnetic saturation fields, underscoring the decisive influence of oxygen stoichiometry and crystalline perfection.

To give an example of these films’ potential applicability, we consider a vortex in a superconducting sample with a penetration depth of about 100 nm which is typical for thin films. At a distance of about 200 nm of the superconductor’s surface where an indicator film could reasonably be positioned using flip-chip stacking, a magnetic field anomaly of some 0.1 mT can be expected due to the vortex. Using a film with the parameters of sample 8 of this work together with an illumination of wavelength of 532 nm and a power of  $1 \mu\text{W}$  which is expected to conserve the superconducting properties of the sample<sup>19</sup>, we estimate that a cross-polarizer setup would yield a signature of about 1 pW of optical power anomaly due to the presence of the vortex. This power is well above the electronic detection noise of most modern photodiodes. Assuming that the cross-polarizer setup leaks 1% of the  $1 \mu\text{W}$  reflected intensity, the shot-noise from that parasitic signal would be of the order of  $50 \text{ fW} / \sqrt{\text{Hz}} \ll 1 \text{ pW}$ , setting a sensitivity estimate well sufficient to detect the signature from a single vortex, although this estimation assumes that the magneto-optical coupling retains its value at lower temperature.

To conclude, we have shown that PLD-growth optimization of LuBiIG films establishes them as benchmark materials for next-generation magneto-optical imaging and field-sensing technologies.

## ACKNOWLEDGEMENTS

We thank Lars Peeters, Junyoung Hyun and Sreeveni Das for their help and guidance on various characterization techniques. We acknowledge the facilities and technical support of Otaniemi research infrastructure for Micro and Nanotechnologies (OtaNano). We also acknowledge the financial support of the Finnish Ministry of Education and Culture through the Quantum Doctoral Education Pilot Program (QDOC VN/3137/2024-OKM-4) and the Research Council of Finland through the Finnish Quantum Flagship project (project number 358877, Aalto University). L. M. d. L. acknowledges funding from the Research Council of Finland (project number 338565).

## CONFLICTS OF INTEREST

The authors have no conflicts to disclose.

## AUTHOR CONTRIBUTION

**Megan H. Dransfield:** Formal analysis (equal), Investigation (equal), Writing - original draft (lead), Writing - review and editing (equal). **Lukáš Flajšman:** Conceptualization (supporting), Formal analysis (equal), Investigation (equal), Writing - review and editing (equal), Funding acquisition (supporting), Resources (lead). **Matthijs H. J. de Jong:** Writing - review and editing (equal), Investigation (equal), Supervision (equal). **Sebastiaan van Dijken:** Supervision (supporting), Resources (supporting), Writing - review and editing (equal). **Laure Mercier de Lépinay:** Conceptualization (lead), Funding acquisition (lead), Supervision (equal), Writing - review and editing (equal).

## DATA AVAILABILITY STATEMENT

The data that support the findings of this study are available from the corresponding author upon reasonable request.

## REFERENCES

<sup>1</sup>D. A. Simpson, J.-P. Tetienne, J. M. McCoe, K. Ganesan, L. T. Hall, S. Petrou, R. E. Scholten, and L. C. L. Hollenberg, *Scientific Reports* **6**,

- 10.1038/srep22797 (2016).
- <sup>2</sup>F. S. Wells, A. V. Pan, S. Wilson, I. A. Golovchanskiy, S. A. Fedoseev, and A. Rozenfeld, *Superconductor Science and Technology* **29**, 035014 (2016).
- <sup>3</sup>P. E. Goa, H. Hauglin, Å. A. F. Olsen, M. Baziljevich, and T. H. Johansen, *Review of Scientific Instruments* **74**, 141 (2003).
- <sup>4</sup>L. Dorosinskiy and S. Sievers, *Sensors* **23**, 4048 (2023).
- <sup>5</sup>S. Tsunashima, *Journal of Physics D: Applied Physics* **34**, R87 (2001).
- <sup>6</sup>M. H. Kryder, *Journal of Applied Physics* **57**, 3913 (1985).
- <sup>7</sup>K. Srinivasan and B. J. H. Stadler, *Optical Materials Express* **12**, 697 (2022).
- <sup>8</sup>D. Jalas, A. Petrov, M. Eich, W. Freude, S. Fan, Z. Yu, R. Baets, M. Popović, A. Melloni, J. D. Joannopoulos, M. Vanwolleghem, C. R. Doerr, and H. Renner, *Nature Photonics* **7**, 579 (2013).
- <sup>9</sup>Y. Nakamura, S. B. S. Chauhan, and P. B. Lim, *Photonics* **11**, 931 (2024).
- <sup>10</sup>K. Shinagawa, E. Tobita, T. Saito, and T. Tsushima, *Journal of Magnetism and Magnetic Materials* **177–181**, 251 (1998).
- <sup>11</sup>P. Hansen, C.-P. Klages, and K. Witter, *Journal of Magnetism and Magnetic Materials* **54–57**, 1405 (1986).
- <sup>12</sup>L. E. Helseth, R. W. Hansen, E. I. Il'yashenko, M. Baziljevich, and T. H. Johansen, *Physical Review B* **64**, 174406 (2001).
- <sup>13</sup>T. R. Johansen, F. G. Hewitt, E. J. Torok, and D. L. Fleming, in *AIP Conference Proceedings*, Vol. 29 (AIP, 1976) pp. 580–582.
- <sup>14</sup>P. Hansen, C.-P. Klages, J. Schuldt, and K. Witter, *Physical Review B* **31**, 5858 (1985).
- <sup>15</sup>R. Rojas, C. Krafft, I. Nistor, D. Zhang, and I. D. Mayergoyz, *Journal of Applied Physics* **95**, 6885 (2004).
- <sup>16</sup>P. Hansen, W. Tolksdorf, K. Witter, and J. Robertson, *IEEE Transactions on Magnetics* **20**, 1099 (1984).
- <sup>17</sup>S. D. Silliman, *Bismuth-doped lutetium iron garnet thin films for the MSW-Optical mode interaction*, Master's thesis, Carnegie Mellon University (1992).
- <sup>18</sup>P. Hansen and K. Witter, *Journal of Applied Physics* **58**, 454 (1985).
- <sup>19</sup>I. S. Veshchunov, W. Magrini, S. V. Mironov, A. G. Godin, J.-B. Trebbia, A. I. Buzdin, P. Tamarat, and B. Lounis, *Nature Communications* **7**, 10.1038/ncomms12801 (2016).
- <sup>20</sup>S. Leitenmeier, A. Heinrich, J. K. N. Lindner, and B. Stritzker, *Journal of Applied Physics* **99**, 10.1063/1.2170057 (2006).
- <sup>21</sup>F. F. Fernández, *Loss circumvention and plasmonic lasing in arrays of magnetic nanodots*, Ph.D. thesis, Department of Applied Physics, Aalto University (2020).
- <sup>22</sup>M. Kataja, *Magneto-optics of plasmonic nickel nanostructures*, Ph.D. thesis, Department of Applied Physics, Aalto University (2016).
- <sup>23</sup>K. Postava, H. Sueki, M. Aoyama, T. Yamaguchi, C. Ino, Y. Igasaki, and M. Horie, *Journal of Applied Physics* **87**, 7820 (2000).
- <sup>24</sup>K. J. Carothers, R. A. Norwood, and J. Pyun, *Chemistry of Materials* **34**, 2531 (2022).
- <sup>25</sup>S. Thakur, P. Tamarat, A. Rochet, J. Birk, I. S. Veshchunov, M. Bezdard, A. I. Buzdin, J.-B. Trebbia, and B. Lounis, *Optics Express* **31**, 24194 (2023).